

REPORT DOCUMENTATION PAGE

Form Approved
OMB NO. 0704-0188

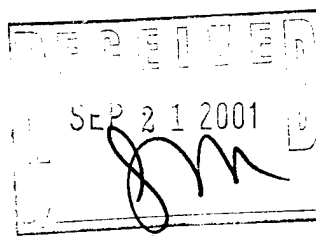
Public Reporting burden for this collection of information is estimated to average 1 hour per response, including the time for reviewing instructions, searching existing data sources, gathering and maintaining the data needed, and completing and reviewing the collection of information. Send comment regarding this burden estimates or any other aspect of this collection of information, including suggestions for reducing this burden, to Washington Headquarters Services, Directorate for information Operations and Reports, 1215 Jefferson Davis Highway, Suite 1204, Arlington, VA 22202-4302, and to the Office of Management and Budget, Paperwork Reduction Project (0704-0188,) Washington, DC 20503.

1. AGENCY USE ONLY (Leave Blank)		2. REPORT DATE September 18, 2001		3. REPORT TYPE AND DATES COVERED Final Technical Report 4/1/98 - 6/30/2001	
4. TITLE AND SUBTITLE FILM SYNTHESIZED RARE EARTH TRANSITION METAL PERMANENT MAGNET SYSTEMS				5. FUNDING NUMBERS Grant No. DAAG55-98-1-0172	
6. AUTHOR(S) Fred. J. Cadieu					
7. PERFORMING ORGANIZATION NAME(S) AND ADDRESS(ES) Physics Department, Queens College of CUNY Flushing, NY 11367				8. PERFORMING ORGANIZATION REPORT NUMBER	
9. SPONSORING / MONITORING AGENCY NAME(S) AND ADDRESS(ES) U. S. Army Research Office P.O. Box 12211 Research Triangle Park, NC 27709-2211				10. SPONSORING / MONITORING AGENCY REPORT NUMBER Proposal No. 37186-MS ✓ 7	
11. SUPPLEMENTARY NOTES The views, opinions and/or findings contained in this report are those of the author(s) and should not be construed as an official Department of the Army position, policy or decision, unless so designated by other documentation.					
12 a. DISTRIBUTION / AVAILABILITY STATEMENT Approved for public release; distribution unlimited.				12 b. DISTRIBUTION CODE	
13. ABSTRACT (Maximum 200 words) Specific results of this research include five unique results. 1. The elucidation of the concept of a growth coherence region as being pivotal for the growth of textured polycrystalline films. This concept allows the prediction of what texture modes would be possible for any new system that may be discovered. 2. For the very first time it was demonstrated that pulsed laser deposition can be used to grow highly textured high coercivity rare earth transition metal films with magnetic properties comparable to the best sputtered films. 3. It was shown that the simultaneous use of sputtering and pulsed laser deposition methods can be used to grow nanophase dispersed films with special magnetic and other properties. 4. A new type of magnetoresistive magnetic memory element operable at room temperature was demonstrated for specially deposited La-manganite films when used in conjunction with another magnetic film element. 5. A method was invented whereby particulate free films of a great many substances can be deposited by pulsed laser deposition.					
14. SUBJECT TERMS High Energy Product Magnetic Materials, Magnetic Films, Sputtered Magnetic Films, SmCo Based Films, Pulsed Laser Deposition, Diamond Like Carbon Films				15. NUMBER OF PAGES 39	
				16. PRICE CODE	
17. SECURITY CLASSIFICATION OR REPORT UNCLASSIFIED	18. SECURITY CLASSIFICATION ON THIS PAGE UNCLASSIFIED	19. SECURITY CLASSIFICATION OF ABSTRACT UNCLASSIFIED	20. LIMITATION OF ABSTRACT UL		

NSN 7540-01-280-5500

Standard Form 298 (Rev.2-89)
Prescribed by ANSI Std. Z39-18
298-102

20011023 051



FILM SYNTHESIZED RARE EARTH TRANSITION METAL PERMANENT MAGNET SYSTEMS

Final Technical Report

**F. J. Cadieu
Physics Department
Queens College of CUNY
Flushing, NY 11367**

September 18, 2001

U. S. Army Research Office

Grant No. DAAG55-98-1-0172
April 1, 1998 to June 30, 2001

Queens College of CUNY and Research Foundation of CUNY

APPROVED FOR PUBLIC RELEASE;

DISTRIBUTION UNLIMITED.

The views, opinions, and/or findings contained in this report are those of the author and should not be construed as an official Department of the Army position, policy, or decision, unless so designated by other documentation.

FILM SYNTHESIZED RARE EARTH TRANSITION METAL PERMANENT MAGNET SYSTEMS

Final Technical Report

**F. J. Cadieu
Physics Department
Queens College of CUNY
Flushing, NY 11367**

September 18, 2001

U. S. Army Research Office

Grant No. DAAG55-98-1-0172
April 1, 1998 to June 30, 2001

Queens College of CUNY and Research Foundation of CUNY

APPROVED FOR PUBLIC RELEASE;

DISTRIBUTION UNLIMITED.

The views, opinions, and/or findings contained in this report are those of the author and should not be construed as an official Department of the Army position, policy, or decision, unless so designated by other documentation.

FILM SYNTHESIZED RARE EARTH TRANSITION METAL PERMANENT MAGNET SYSTEMS

Table of Contents

List of Figures and Illustrations	3
<u>Body of Report:</u>		4
A. Statement of the Problem Studied	...	5
B. Summary of the Most Important Results		6
I. Textured Film Growth via Sputtering, Epitaxy, and PLD	...	6
II. Successes in the Growth of Highly Textured Permanent Magnet Films by Pulsed Laser Deposition	...	13
III. Enhanced Magnetic Properties of SmCo ₅ Nanophase Composites Made By Simultaneous Pulsed Laser Deposition and Sputtering	...	21
IV. Advances in Magnetoresistive Magnetic Memory Structures	...	23
V. The Growth of Particulate Free Films by a newly invented deposition method using a pulsed laser	...	29
Bibliography for Summary of the Most Important Results	...	32
C. Papers Directly Resulting From U. S. Army Research Office Support As A Part of This Grant	...	35
Invited Longer Papers, Book Chapters, and Review Articles	...	35
D. Scientific Personnel	...	36
E. Degrees Awarded as a Part of This Program	36
F. Report of Inventions (By Title Only)	...	36

List of Figures and Tables

	Page
Table 1. Hard Magnet System Texture Considerations. An important new concept is the introduction of a growth coherence area as a requirement for the growth of textured films.	10
Table 2. The crystal texturing and room temperature intrinsic coercivities for SmCo based uniaxial films deposited by different methods are summarized.	13
Fig. 1. Hysteresis loops as measured at 293 K are shown for a SmCo shadow deposited film deposited with a pulse energy of 1200 mJ with a repetition rate of 14 Hz. In plane loops for magnetizing fields of ± 20 kOe and ± 90 kOe are shown. The perpendicular to the plane loop is closed. This film was PLD deposited from a SmCo ₅ target on to 375 °C alumina substrate at a pressure of 100 mTorr Ar.	16
Fig. 2. SEM micrographs are shown for shadow deposit (left) and non-shadow deposit (right) regions for a CaCu ₅ -type structure film deposited with 1200 mJ pulses and a pulse rate of 16 Hz.	17
Fig. 3. An x-ray diffraction trace for the non-shadow region of the film of Fig. 1 is shown which indicates (110) and (111) texturing. X-Ray indexed as CaCu ₅ -type structure film.	18
Fig. 4. Hysteresis loops are shown for SmCo ₅ film deposited by PLD directly onto a silicon substrate heated to 375 °C	19
Fig. 5. An x-ray diffraction trace, Cu K α radiation, is shown for the SmCo ₅ film of Fig. 4 that was directly crystallized by PLD onto a silicon substrate.	19
Fig. 6. The intrinsic coercivity is shown for a series of SmCo films shadow deposited by PLD onto alumina substrates held at 375 °C in 100 mTorr Ar. All points were measured at 295 K except for those indicated by Δ , which were measured at 140 K. The points indicated by O were deposited with $\lambda = 193$ nm with pulse energies of 500-650 mJ. The points indicated by \square were deposited with $\lambda = 248$ nm with pulse energies of 1000-1250 mJ.	19
Fig. 7. Room temperature hysteresis loops are shown for a PLD SmCo ₅ plus Al sputter film containing Sm 15.8 at.%, Co 74.5 at.%, and Al 9.7 at.%. The intrinsic coercivity was 9.9 kOe.	21
Fig. 8. Room temperature hysteresis loops are shown for a high coercivity PLD SmCo ₅ sample plus simultaneous Co sputter deposition. The RT in plane intrinsic coercivity was 9.5 kOe.	21

- Fig. 9. Room temperature hysteresis loops are shown for a lower coercivity PLD SmCo_5 sample plus simultaneous Co sputter deposition. The RT in plane intrinsic coercivity was 3.4 kOe. 22
- Fig. 10. The intrinsic coercivities measured at room temperature following heating for 30 minutes in air at various temperatures are shown for PLD SmCo plus Al films, diamonds, PLD SmCo plus Co, crosses, and PLD SmCo_5 only films, circles. 22
- Fig. 11. This figure indicates the range of R vs T variation for high laser pulse energy LaSrMnO PLD deposited films. Traces (a), (b), and (c) are for shadow deposited films at high laser pulse energies. Trace (d) was for the non-shadow deposited region of the same substrate as trace (c). The temperatures corresponding to the maximum resistance for each trace are indicated. 24
- Fig. 12. X-ray diffraction traces are shown for the shadow, trace (a), and non-shadow regions, trace (b), corresponding to traces (c) and (d) respectively of Fig. 1. The shadow region trace has been displaced by 500 counts to separate the traces. Trace (c) is for the shadow region of a (110) and (111) mixed texture high pulse shadow deposited textured film. Trace (c) has been offset by 1500 counts. Peaks due to the polycrystalline alumina substrate are denoted by S. 25
- Fig. 13. The low field MR anisotropy for a (110) textured film is shown versus applied magnetic fields applied in plane, parallel and perpendicular to current, and perpendicular to plane as at measured at 293 K are shown. The curves were hysteretic with the peaks lagging the applied field values. A bridge output of 100 mV corresponds to a resistance change $\Delta R/R \approx 2.2\%$. 26
- Fig. 14. The low field MR anisotropy for a mixed (111) + (110) textured film is shown versus applied magnetic fields applied in plane, parallel and perpendicular to current, and perpendicular to plane as at measured at 293 K. 26
- Fig. 15. The bridge output, cycled three times, versus applied magnetic field for a LaSrMnO patterned film strip biased by a small bias magnet parallel to the strip is shown. The inset shows that the film strip current, bias magnet, and external field are all aligned parallel to each other. The vertical line is located at the $H = 0$ position. 27
- Fig. 16. The upper graph shows the pulse train of applied field values used to produce the zero applied field voltage state values of the lower panel. The zero applied field voltage levels differed by 18 mV. 27
- Fig. 17. Optical constants versus wavelength are shown for two laser carbon ion deposited films on silicon substrates, samples 051501 and 051701, along with a calibration film deposited by filtered cathodic arc deposition, a-sft. 31

FILM SYNTHESIZED RARE EARTH TRANSITION METAL PERMANENT MAGNET SYSTEMS

**F. J. Cadieu
Physics Department
Queens College of CUNY
Flushing, NY 11367**

Statement of Problem

This grant was concerned with the optimization of film growth methods for synthesizing highly textured rare earth transition metal permanent magnet systems. The principal results of this research show that highly textured polycrystalline films can be made by both sputtering and pulsed laser deposition methods. In terms of sputtering the critical growth parameters that allow arbitrarily thick highly textured films to be made are the substrate temperature, sputtering gas pressure, and the film deposition rate. It was demonstrated that the controlled growth of textured high coercivity films by pulsed laser deposition requires consideration of three additional growth parameters. These include a filtering method to remove particulates from the pulsed laser generated plume, careful control of the laser pulse repetition rate, and that the laser energy per pulse must exceed a certain threshold value to achieve film coercivities comparable to that realized for sputtered films. Specific results of this research include five unique results.

1. The elucidation of the concept of a growth coherence region as being pivotal for the growth of textured polycrystalline films. This concept allows the prediction of what texture modes would be possible for any new system that may be discovered.
2. For the very first time it was demonstrated that pulsed laser deposition can be used to grow highly textured rare earth transition metal films (demonstrated for SmCo_5 films) with magnetic properties comparable to the best sputtered films.
3. It was shown that the simultaneous use of sputtering and pulsed laser deposition methods can be used to grow nanophase dispersed films with special magnetic and other properties. In this case it was demonstrated that nanophase dispersions of SmCo_5 with aluminum can be made that are stable for heating in air to 300 °C.
4. A new type of magnetoresistive magnetic memory element operable at room temperature was demonstrated for specially deposited La-manganite films when used in conjunction with another magnetic film element.
5. A method was invented whereby particulate free films of a great many substances can be deposited by pulsed laser deposition. It was demonstrated that highly adherent and hard diamond like carbon films can be deposited onto even room temperature substrates by this method.

B. Summary of the Most Important Results

I. Textured Film Growth via Sputtering, Epitaxy, and PLD

As a part of this research program a book chapter titled "Permanent Magnet Films for Applications" was published in an Academic Press series on Magnetic Films for Applications.[1] Parts of that book chapter contained information on the growth of textured magnetic films that had not been previously published. A principal result of that work was the introduction of a growth coherence area as a useful quantity for elucidating when it may be possible to grow films with a particular texture orientation. A particular result was that it is only possible with present methods of sputtering to grow textured films that exhibit a "growth coherence area" of less than $\approx 350 \text{ \AA}^2$. For the $\text{Sm}_2(\text{Co,Fe,Zr,Cu})_{17}$ system an important consequence of this limitation is that it should be possible to grow 2-17 rhombohedral phase films with the crystallographic c-axes splayed about in the substrate plane, but not films that would have the c-axes orientated perpendicular to the substrate plane. Part of these textured film growth considerations are presented here.

There are two basic methods for preparing crystalline films of permanent magnet materials. The first and easiest is to first deposit an amorphous deposit which is subsequently crystallized. Unfortunately the subsequent crystallization of such deposits up to the present time has not been able to produce films with a substantial degree of preferred crystal texturing. In order to realize a higher fraction of the theoretically possible energy density it becomes necessary to synthesize permanent magnet films that exhibit a large degree of preferential or textured crystal growth. Such films have only been synthesized by directly crystallizing the films onto heated substrates and by making use of either process control parameters or substrate film epitaxy. Film texturing through sputter process control will be discussed first. Sputter process control allows the growth of textured films onto polycrystalline substrates. If suitable boundary adhesion layers are used, highly textured films from approximately 0.05 \mu m to greater than 100 \mu m thickness have been grown by this method.

Textured film growth requires that the energy and momentum of the deposited atoms be controlled to avoid disrupting the growth of a particular texture mode. In sputtering this is

accomplished by using sufficiently high sputtering gas pressures so that the deposited atoms undergo collisions before reaching the substrate position. Various thermalization methods employing inert gases or mixtures such as Ar, Ar-Kr, Ar-Xe, Kr, and Xe have been used to enhance the degree of preferential texturing that the permanent magnet films exhibit. The high mass Xe atoms are useful in two respects. One is that Xe closely approximates the mass of the rare earths to provide efficient momentum transfer per collision. The other is that the lower mass transition metals such as Co and Fe are on average scattered through large angles by collisions with Xe atoms so that a composition change from the target to deposited films can be effected. For the sputtering of SmCo based films it was shown that comparable thermalization profiles for the sputtered atoms arriving at the substrates can be obtained in 130 mTorr Ar, 60 mTorr Ar50%Xe, and 30 mTorr Xe.[2] Full texturing was not realized with an Ar sputtering gas until the sputtering gas pressure was increased to 60 mTorr. X-Ray diffraction traces with logarithmic y-axes showed the complete absence of grains with crystallite c-axes skewed out of the film plane. For SmCo based films sputtered in Ar50%Xe mixtures and a constant substrate temperature of 345 °C changing the sputtering gas pressure from 15 to 105 mTorr changed the Sm at.% in the deposited films from 12 to 17 at.%. [3] For similar SmCo based films sputtered in 60 mTorr Ar50%Xe changing the substrate temperature from 240 to 520 °C reduced the collected film Sm at.% from 16 to 13 at.%. [3] If the direct growth of crystalline permanent magnet films is considered, then it is desirable that one or more process control parameters be effective in causing preferentially textured films to be synthesized. By direct growth is meant that the magnetic material is to be deposited directly onto a substrate, which can be either polycrystalline or single crystal, which is held at a sufficiently high temperature so that the magnetic material crystallizes upon deposition. Several process control parameters can be utilized to produce magnetic films with specifically textured structures to effect the resultant magnetic properties of the films. These texture control parameters operate independent of any substrate-film epitaxy considerations. Three principal process control parameters can be used to synthesize preferentially textured magnetic films.[4] Only one of these requires that the material being deposited be ferromagnetic at the deposition temperature. The other

two principally affect the relative probability for the growth of crystallites with various lattice parameter considerations. The three principal process considerations are:

- (1.) the demagnetization energy required to produce a net magnetization perpendicular to the film plane versus in the film plane,
- (2.) c/a ratio effects, and
- (3.) the crystal structure stacking length perpendicular to the substrate plane.

For texture control 1 to be effective requires that the anisotropy energy per grain volume be greater than $k_B T$ at the temperature of interest. This condition is normally well satisfied for Co based hard magnetic materials, but can only be marginally satisfied for Fe based hard magnets. During the direct crystallization of films onto heated substrates, certain textures are favored from an initial random growth pattern. Once some larger seed grains become formed, there is a tendency for these grains to act as seeds for the subsequent film growth. It has only been possible to deposit relatively thick permanent magnet films, $\geq 1 \mu\text{m}$, with magnetic energy densities greater than about 6 MGOe by directly crystallizing the rare earth transition metal compounds onto heated substrates. At least one of the texture controlling switches can then be used to preferentially align the crystallite c-axes and achieve magnetic energy densities greater than that possible for an isotropic deposit. Techniques such as selectively thermalized sputtering allow sensitive relative growth probability factors to be propagated as the film thickness grows.[5-19]

Predominantly factor (1.) allows textured SmCo_5 and SmCo based TbCu_7 films to be synthesized such that the c-axes of all the crystallites are aligned onto the substrate plane. Similarly factors (2.) and (3.) have allowed ThMn_{12} type films to be synthesized into either a (002) or (222) textured modes in a controlled fashion. Factor (3.) has also allowed SmCo_5 and SmCo TbCu_7 films to be synthesized into either a (200) or (110) texture modes in a controlled fashion. When textured films are grown onto polycrystalline substrates, then the growth of crystallites with certain orientations becomes dynamically favored due to a certain choice of sputtering parameters. A necessary condition is that the growth be coherent over a certain minimal surface region to allow the structure to be

replicated. The usual permanent magnet phases and the crystal structure parameters that influence texturing are summarized in Table 1. Texture modes indicated by (xy0) have the c-axes aligned onto the substrate plane. Texture modes (00z) have the c-axes perpendicular to the substrate plane. Lateral diffusion of the surface atoms due to the heated substrate surface disrupt the growth coherence to limit the textures that can be grown. The growth region definitions chosen are believed to provide a useful measure of the relative surface sizes required to grow the different structures. At the present time textured films have been synthesized which require a surface coherence region of less than about 300 \AA^2 . Thus ordered rhombohedral films of the $\text{Sm}_2(\text{Co,Fe,Zr,Zr})_{17}$ system with c-axes in-plane texture have been synthesized for the (xy0) mode, but textured films of the 2-17 phase have not been grown with the (00z) texture.[68] Note that for 2-17 (00z) textured films a surface coherence region during the growth of 393 \AA^2 would be required. For a given structure textures tend to grow favorably that require the smaller growth coherence region. Thus for SmCo_5 textured growth with c-axes skewed out of the film plane is usually observed and such films exhibit perpendicular anisotropy.[64] Other phases that would require unusually large growth coherence regions, such as the very high coercivity $\text{Sm}_5(\text{Fe,Ti})_{17}$, $H_c \approx 50 \text{ kOe}$ at room temperature, have only been formed by the subsequent crystallization of amorphous deposits, but not as directly crystallized textured films.[20-22]

Table 1. Hard Magnet System Texture Considerations. An important new concept is the introduction of a growth coherence area as a requirement for the growth of textured films.

System	Structure	Minimum Area for Growth
$\text{Sm}_5(\text{Fe,T})_{17}$	Hexagonal $a = 20.06 \text{ \AA}$ $c = 12.28 \text{ \AA}$ $c/a = 0.612$	(00z): $6 \cdot a^2 \cdot \sin 60^\circ = 2091 \text{ \AA}^2$ (xy0): $2 \cdot a \cdot c = 493 \text{ \AA}^2$
SmCo_5	Hexagonal $a = 5 \text{ \AA}$ $c = 4 \text{ \AA}$ $c/a = 0.8$	(00z): $6 \cdot a^2 \cdot \sin 60^\circ = 130 \text{ \AA}^2$ (xy0): $2 \cdot a \cdot c = 40 \text{ \AA}^2$
SmCo_3	Hexagonal $a \approx 5 \text{ \AA}$ $c \approx 24 \text{ \AA}$ $c/a = 4.8$	(00z): $6 \cdot a^2 \cdot \sin 60^\circ \sim 130 \text{ \AA}^2$ (xy0): $2 \cdot a \cdot c \sim 240 \text{ \AA}^2$
SmCo based	Hexagonal TbCu_7 $a = (5-8) \text{ \AA}$ $c = 4 \text{ \AA}$ $c/a = \sim 0.8$	(00z): $6 \cdot a^2 \cdot \sin 60^\circ \sim 130 \text{ \AA}^2$ (xy0): $2 \cdot a \cdot c \sim 40 \text{ \AA}^2$
$\text{Sm}_2\text{Co}_{17}$ $\text{Sm}_2\text{Fe}_{17}$	Ordered Rhombohedral $a = 8.7 \text{ \AA}$ $c = 12.2 \text{ \AA}$ $c/a = 1.40$	(00z): $6 \cdot a^2 \cdot \sin 60^\circ = 393 \text{ \AA}^2$ (xy0): $2 \cdot a \cdot c = 212 \text{ \AA}^2$
$\text{Sm}(\text{Fe,T})_{12}$	Tetragonal $a = 8.50 \text{ \AA}$ $c = 4.79 \text{ \AA}$ $c/a = 0.56$	(00z): $4 \cdot a^2 = 289 \text{ \AA}^2$ (xy0): $2 \cdot a \cdot c = 81 \text{ \AA}^2$
$\text{Nd}_2\text{Fe}_{14}\text{B}$	Tetragonal $a = 8.81 \text{ \AA}$ $c = 12.2 \text{ \AA}$ $c/a = 1.38$	(00z): $4 \cdot a^2 = 310 \text{ \AA}^2$ (xy0): $2 \cdot a \cdot c = 215 \text{ \AA}^2$

Textured films have generally been sputter deposited at rates of less than 10 \AA/sec . To maintain the growth of a specific texture mode the surface mobility of the atoms over the growth region must be small. It is argued that at the comparatively low deposition rates, the surface mobility is

sufficiently high so that there is a maximum growth region size over which structure coherence can be maintained. It should be noted that the substrate deposition temperatures are well below the melting points for the phases of interest. Consequently once the surface is covered, the atomic positions are well fixed. It should be noted that large growth region phases such as the 5-17 and 2-17 phases can be readily formed by the subsequent crystallization of originally amorphous sputter deposits.[22,23] In that case there is no heated surface region over which growth coherence needs to be maintained.

If the stacking distance for growth repetition is represented by s and the film growth rate by R then the time defined by $s/R = \tau$ defines a characteristic growth time for the film. The number of growth sites in a region required to define a crystallite is given by $A/(\pi r^2) = n$ where A is the area of the growth coherence region required to define a crystallite texture. If we let v_{pl} be a site hopping speed for motion in the plane, then the atom positions need be defined to an approximate extent

$$\tau \cdot n \cdot v_{pl} \leq d$$

$$\tau \cdot (A/(\pi r^2)) \cdot v_{pl} = (s/R) \cdot (A/(\pi r^2)) \cdot v_{pl} \leq d$$

where d is a mean atomic position spacing. This expression agrees with the observations that is difficult to grow textured films with normal sputtering rates for large coherence regions and large stacking distances. Whether d or several d should be used to allow for crystallites with defects is a minor point and shouldn't change the functional form of the expression. If rates can be substantially increased, it also gives the expectation that crystallites corresponding to larger spatial regions become a growth possibility. At higher substrate temperatures v_{pl} increases so that higher rates may be required to maintain the growth of longer stacking sequence textures as has been observed for the growth of the variable texture ThMn_{12} type films.

It is most useful to illustrate these considerations with examples for films of a particular crystallographic type. The most representative permanent magnet film systems are SmCo_5 , crystallizing in the 1-5 CaCu_5 structure, and Sm-Co based systems crystallizing into the disordered 1-5 TbCu_7 structure. These structures have very similar hexagonal lattice constants with $a \sim 5 \text{ \AA}$, and $c \sim 4 \text{ \AA}$. They differ in that the disordered 1-5 structure allows certain pairs of transition metal atoms to occupy rare earth sites and thus are transition metal rich. This allows the possible magnetization to be

enhanced due to the higher transition metal content at the expense of magnetic anisotropy. The usual result of this is that true SmCo_5 structured films exhibit greater intrinsic coercivities than disordered TbCu_7 -type structure films. As the fraction of transition metal atom pair substitutions is increased, several distinct transformation related phases can be formed.[24] Ordered phases occur for every third rare earth atom in the parent CaCu_5 -type structure replaced by a transition metal dumbbell pair. For the light rare earths this results in the 2-17 rhombohedral $\text{Th}_2\text{Zn}_{17}$ -type structure phase, and for the heavy rare earths the 2-17 hexagonal $\text{Th}_2\text{Ni}_{17}$ -type structure phase. For every other rare earth atom replaced by a transition metal dumbbell pair, the 1-12 or ThMn_{12} -type structure compounds are formed. The disordered TbCu_7 has a higher saturation magnetization because of the higher transition metal concentration. The transition metal atom dumbbell pairs align parallel to the c -axis which results in a slight contraction of the a parameter of the TbCu_7 cell relative to that of the CaCu_5 cell. These Sm-Co based systems are strong uniaxial permanent magnet systems over the entire temperature range up to the Curie points. Directly crystallized SmCo based films crystallized into either the CaCu_5 ordered structure or the TbCu_7 -type disordered structure tend to have the crystallite c -axes randomly splayed onto the substrate plane. Thermalized sputtering has been used to grow films that essentially have all the crystallite c -axes aligned onto the film plane. For uniaxial systems a comparison of the magnetic hysteresis loops measured with the applied field in the film plane versus perpendicular to the film plane provide a very good indicator of the degree of c -axes in plane alignment. The specific qualitative indicator is the smallness of the perpendicular to in plane remanent ratio for hysteresis loops measured perpendicular to and in the film plane. Perpendicular to in plane remanent ratios as small as 0.05 are relatively easier to produce for CaCu_5 -type structure films that exhibit higher magnetocrystalline anisotropy and higher intrinsic coercivities than for TbCu_7 -type structure films. The c/a ratios for both of these structures are very close to 0.8. This value of c/a ratio does not differ from unity by a substantial amount to be operative as a texture control factor relative to the demagnetization energy. For the Sm-Co system each of the compounds; ordered phase SmCo_5 , disordered transition metal substituted TbCu_7 phase, and ordered $\text{Sm}_2\text{Co}_{17}$ phases are uniaxial. The magnetic behaviors are similar but with a reduced anisotropy from the extremely high H_A for SmCo_5 of 500 kOe, to a relatively low

value for $\text{Sm}_2\text{Co}_{17}$. The Curie point for SmCo_5 is very high at about 700 °C with somewhat higher temperatures observed for more transition metal rich Sm-Co films. Recently SmCo based TbCu_7 -type disordered structures have come into prominence as high temperature permanent magnet materials.[25,26] Table 2 is a summary of room temperature coercivity values obtained for SmCo based films deposited by different methods.

Table 2. The crystal texturing and room temperature intrinsic coercivities for SmCo based uniaxial films deposited by different methods are summarized.

	Texture	H_c (kOe)	Ref.
SmCo CaCu_5 -type	(110) sputter proc. Control	up to 23	13
	(200) sputter proc. Control	up to 12	13
	(110) dom. by PLD	up to 22.5	27
	(110) epitaxial, Cr(100) on MgO(100)	≈ 31	28
	(200) epitaxial, Cr(211) on MgO(110)	10-40, $\propto 1/t$ to 75Å	28
	random, subsequent Cryst.	≈ 36	7
Sm(Co,Fe,Cu,Zr) Sm \approx at.%, Fe <30 at.% - TbCu_7 -type	(200), (110) mixed	8-10	29
Sm(Co,Fe,Cu,Zr) Sm >17 at.% - CaCu_5 - type	(110), (200) mixed	12	30
Sm(Co,Fe,Cu,Zr) Sm \approx 13 at.%, Fe \approx 30 at.% rhombohedral 2- 17 type,	(300)	8, subsequent to deposition annealing required	31

II. Successes in the Growth of Highly Textured Permanent Magnet Films by Pulsed Laser Deposition

At the beginning of this research effort no films grown by pulsed laser deposition, PLD, with coercivities greater than about 1 kOe had

been reported. Several new considerations and growth parameters not encountered in sputtering were defined for the first time that allowed the

growth of fully textured films of SmCo_5 with properties similar to the best films grown by sputtering.

SmCo based films directly crystallized onto moderately heated polycrystalline substrates have been synthesized by pulsed laser deposition, PLD, with room temperature intrinsic coercivities greater than 20 kOe. The crystallite c-axes are fully aligned onto the substrate plane. In a previous paper it was demonstrated for the first time that moderately high coercive force SmCo based films could be synthesized by pulsed laser deposition, PLD.[32] It was shown that for a laser pulse energy of 600 mJ that the coercive force was sharply peaked as a function of pulse repetition rate. A maximum H_c of 11.3 kOe was attained for pulse rates in the vicinity of 10-15 Hz. For the present study, laser pulse rates previously shown capable of producing high coercivity films have been used. In that case a laser wavelength of 193 nm was used. The moderately high intrinsic coercivities were observed only for the shadow deposited regions of the substrates. Highly c-axes in plane textured polycrystalline films have usually been made by

using sputter process control to grow films with thicknesses out to at least 120 μm . [5,6,8,33] Such films have the crystallite c-axes nearly randomly aligned onto the substrate plane. Buffer layers are necessary to grow relatively thick films, but in principle arbitrarily thick films of highly aligned SmCo deposits can be grown by this method. In contrast to this, highly aligned thin films with thicknesses of less than 0.1 μm have been grown by using substrate film epitaxy.[28,34] The thicker films as grown by sputter process control onto polycrystalline substrates are generally more suited to device applications. There have been few other reports of rare earth transition metal magnetic films as grown by PLD and mostly confined to $\text{Nd}_2\text{Fe}_{14}\text{B}$. [35,36] Coercivities have either not been reported,⁸ or were low at less than 1 kOe.[36]

Although the time averaged deposition rates of sputter and PLD deposited films are comparable, material is ejected in PLD only during a series of pulses of very short time duration compared to the time between pulses.[37] This means that the relative mobility of deposited surface atoms is very much less for PLD than for sputtering since a complete

monolayer can be deposited per pulse. PLD deposition from rare earth transition metal targets presents special problems since the deposition plume consists of a range of particle sizes ranging from individual atoms to clusters and larger sized particulates. The laser beam often causes surface roughening for metallic targets that leads to droplet ablation.[38] For the SmCo targets used in this study a large profusion of relatively uniform size droplets was observed in the non-shadowed deposits. A laser wavelength of 248 nm has been used in this study which allowed the laser pulse energy to be increased up to 1250 mJ. For these metallic targets the laser pulse energy is believed to play a more dominant role than the laser wavelength over this range. The high laser pulse energies used in this study have made the shadow and non-shadowed regions distinctly different. In this paper we have investigated the relative magnetic properties of PLD shadow deposition versus non-shadow deposition.

Pulsed laser deposition, PLD, utilizing a Lambda Physik 305Fi excimer laser has been used to deposit SmCo based films from a set of bulk compound targets. Films have been deposited using wavelengths of 248 nm with

pulse energies from 500 to 1250 mJ, and 193 nm with pulse energies of 500-650 mJ, at 5-50 Hz, with an estimated pulse width of 15 ns. A shadow mask has been used to shield part of the substrate during the PLD process. In this manner the magnetic properties, as well as the number of particulates reaching the substrate, in and out of the shadow region could be observed. Most of the films discussed here have been grown using a substrate temperature of 375 °C in 100 mTorr argon. In most runs films have been simultaneously deposited onto alumina and silicon substrates. Very little difference was observed in the film magnetic properties for these different substrate materials. Film compositions were determined using electron excited x-ray analysis in a scanning electron microscope, SEM. The film composition measurements were calibrated against known bulk composition standards. The SmCo films discussed in this paper contained 20-22 at.% Sm. Magnetic measurements were made using high field, ± 90 kG, and low field, ± 19 kG, vibrating sample magnetometers. All magnetic measurements were made on as deposited films without any subsequent heat treatments.

Figure 1 shows room temperature hysteresis loops for a SmCo film shadow deposited from bulk SmCo₅ targets by high pulse energy PLD using $\lambda = 248$ nm at pulse energy 1200 mJ with a 14 Hz repetition rate.[27] The deposit was directly crystallized onto alumina substrates at 375 °C in 100 mTorr Ar to effect deposition behind the shadow. In plane hysteresis loops for measurement fields up to ± 20 kOe, and ± 90 kOe are shown. This film was ≈ 1 μ m thick. Because of uncertainties in the exact thickness, the experimental emu value that depends upon the film thickness as well as the film area has been given as the ordinate. For such films the low field measurements yield only minor loops that are generally offset because the films exhibit some remanent moment as removed from the PLD system. For this film the high field measurements indicated an in plane intrinsic coercive force of 22.5 kOe. For this film measurements made perpendicular to the film plane, as shown for the low field measurements in Fig. 1 indicated only skewed lines with no detectable coercivity or perpendicular remanence. Films of the type shown in Fig. 1 have only been synthesized by using high laser pulse energies over a narrow

range of laser pulse repetition rates. Previously it was shown for a laser pulse energy of 600 mJ, $\lambda = 193$ nm, that the attainable coercivities exhibited a maximum of 11.3 kOe for a pulse repetition rate of ≈ 10 -15 Hz. The high pulse energy films have now exhibited twice this coercivity value. Films directly crystallized onto alumina and silicon substrates exhibited very nearly the same magnetic properties when simultaneously deposited in the same deposition run. For in-plane hysteresis loops the average value of M_r/M_s was 0.86 for ten high coercivity films.

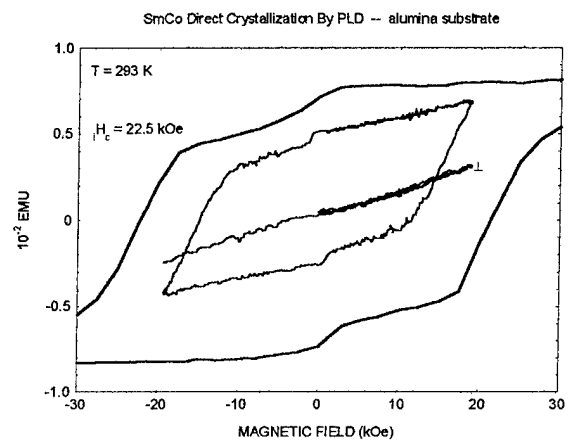


Fig. 1. Hysteresis loops as measured at 293 K are shown for a SmCo shadow deposited film deposited with a pulse energy of 1200 mJ with a repetition rate of 14 Hz. In plane loops for magnetizing fields of ± 20 kOe and ± 90 kOe are shown. The perpendicular to the plane loop is closed. This film was PLD

deposited from a SmCo_5 target on to 375°C alumina substrate at a pressure of 100 mTorr Ar.

As we previously reported, high coercivity films have only been observed for shadow deposited films. Figure 2 shows SEM micrographs for the film of Fig. 1 in and out of the shadow region. Visually both regions were

mirror-like, but the SEM examination shows the film structure to be very different. The shadow region exhibits a very fine grain structure of $<0.2\ \mu\text{m}$ that is not clearly discernable. In the shadow region only, polishing marks on the underlying substrate were replicated. The non-shadowed deposit shows a mixed deposit consisting of fine and coarse grain sizes. Non-shadowed regions of films made at these high laser pulse energies consisted of a relatively uniform mixture of fine and coarse grained material.

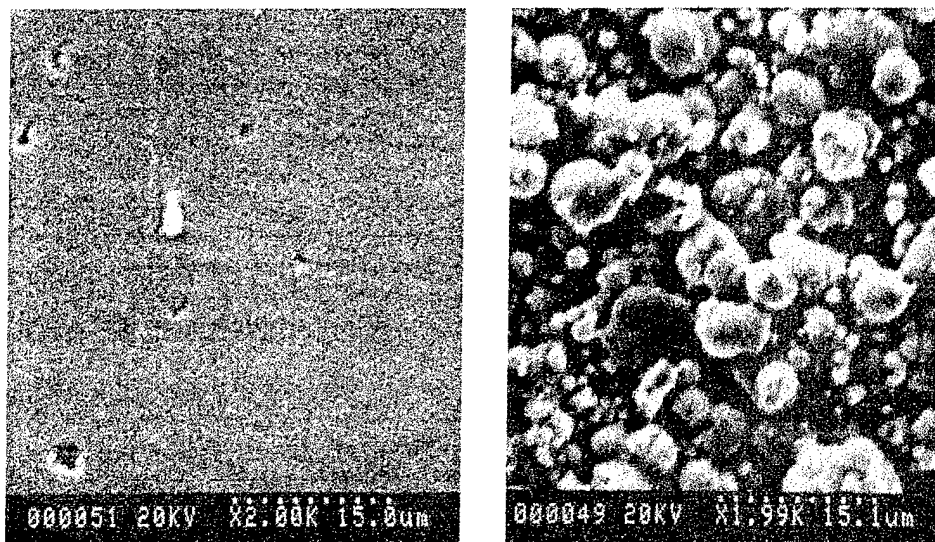


Fig. 2. SEM micrographs are shown for shadow deposit (left) and non-shadow deposit (right) regions for a CaCu_2 -type structure film deposited with 1200 mJ pulses and a pulse rate of 16 Hz.

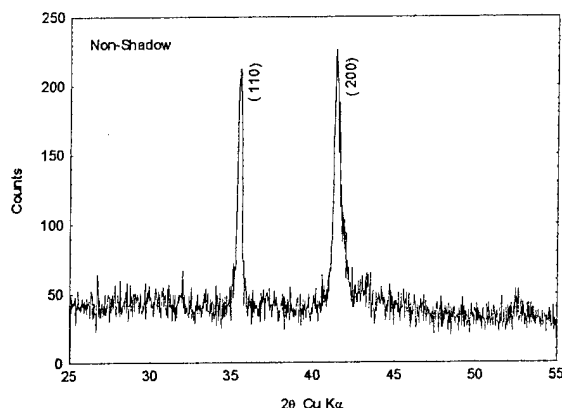


Fig. 3. An x-ray diffraction trace for the non-shadow region of the film of Fig. 1 is shown which indicates (110) and (111) texturing. X-Ray indexed as CaCu_5 -type structure film.

Both shadow and non-shadow regions of the same substrate showed similar x-ray diffraction patterns with the CaCu_5 -type (110) and (200) reflections dominant. Films made at high laser pulse energies did not give any indication of crystallites with c-axes skewed out of the film plane. The shadow region of such films exhibited high coercivities of >20 kOe, and closed perpendicular to the film plane hysteresis loops. Figure 3 shows an x-ray diffractometer trace of the non-shadowed region of Fig. 2. The film in the non-shadow region was $\approx 3 \mu\text{m}$ thick. The larger grained particulates still were c-axes in plane aligned as for the fine grained matrix observed in the shadow region. Judging from the x-ray alone there was the expectation that the non-shadowed deposit should exhibit reasonable

magnetic properties. But this was not the case. The observed non-shadow region hysteresis loops were composite loops indicative of non-coupled fine and coarse grain regions as seen in the non-shadow region SEM micrograph. The observed non-shadow hysteresis loops were constricted near the origin. It should be noted that shadowed regions of the same substrate exhibited high coercivities and single phase type hysteresis loops. Thus contamination did not cause the loop constriction for the non-shadow regions.

It was possible to grow similarly highly textured SmCo_5 films by PLD onto silicon substrates. Hysteresis loops for a SmCo_5 film directly crystallized onto a silicon substrate heated to 375°C in Fig. 4. Figure 5 shows an x-ray trace for the silicon substrate film of Fig. 4 showed that all c-axes are aligned onto the substrate plane.

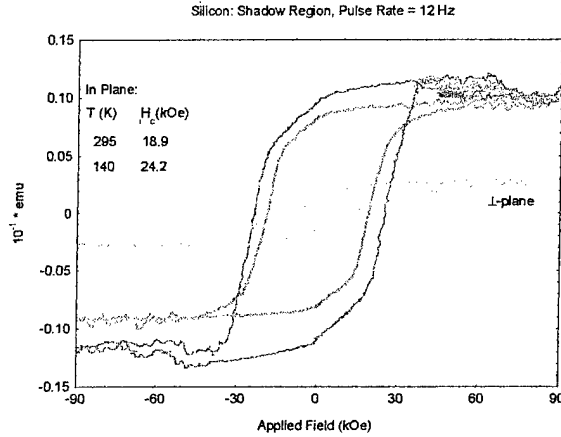


Fig. 4. Hysteresis loops are shown for SmCo_5 film deposited by PLD directly onto a silicon substrate heated to 375 °C.

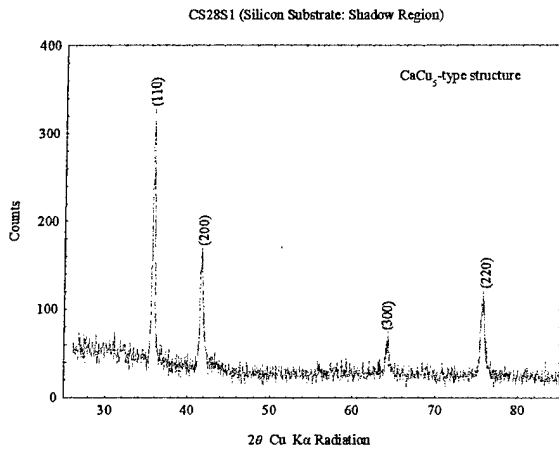


Fig. 5. An x-ray diffraction trace, $\text{Cu K}\alpha$ radiation, is shown for the SmCo_5 film of Fig. 4 that was directly crystallized by PLD onto a silicon substrate.

Figure 6 shows the room temperature H_c versus the laser pulse rate for films made with $\lambda = 193$ nm with pulse energies of 500-650 mJ, and for films made with $\lambda = 248$ nm with pulse energies of 1000-1250 mJ. At lower

temperatures the coercivities increased, as expected, as indicated by the values measured at 140 K. It was necessary to use the higher laser pulse energies, which are only available with $\lambda = 248$ nm, to achieve the higher coercivity values. The laser pulse energy was more crucial than any difference in laser interaction due to the difference in laser wavelength. This was shown by the fact that the region of maximum coercivity was the same as a function of pulse rate for the two wavelengths.

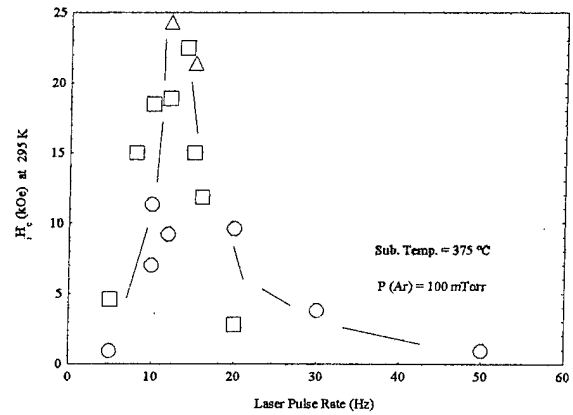


Fig. 6. The intrinsic coercivity is shown for a series of SmCo films shadow deposited by PLD onto alumina substrates held at 375 °C in 100 mTorr Ar. All points were measured at 295 K except for those indicated by Δ , which were measured at 140 K. The points indicated by \circ were deposited with $\lambda = 193$ nm with pulse energies of 500-650 mJ. The points indicated by \square were deposited with $\lambda = 248$ nm with pulse energies of 1000-1250 mJ.[27]

The coarse grains of the non-shadow deposits were too large to exchange spring couple so that composite loops were observed. For the shadow regions, the observed high $M_r/M_s \approx 0.86$ values indicated that the grains were exchange coupled. The expected ratio for independent uniaxial grains with c-axes in-plane alignment is $2/\pi = 0.64$. [5] Pulsed laser ablation from the SmCo_5 targets inherently resulted in atomic as well as larger particulates being ejected from the target. The high laser pulse energies used in this study aided in making the shadow and non-shadowed regions distinctly

different. Shadowing was thus required to obtain uniformly fine grained deposits capable of yielding high coercivities. This conclusion is fully supported by the results of this paper. The high laser pulse energies have also resulted in the deposition of CaCu_2 -type films such that the crystallite c-axes are fully aligned onto the film plane. Uniform fine grained shadow region deposits have been synthesized with intrinsic coercivities of greater than 20 kOe at room temperature.

III. Enhanced Magnetic Properties of SmCo_5 Nanophase Composites Made By Simultaneous Pulsed Laser Deposition and Sputtering

Nanophase dispersions of SmCo_5 in either an Al or Co matrix have been synthesized by using pulsed laser deposition, PLD, to deposit the SmCo aggregated grains while simultaneously sputtering either Al or Co. Shadow deposition as shown in Fig. 2 was necessary to obtain particulate free high coercivity films.[32] It was also necessary to use high laser pulse energies and a very narrow pulse repetition rate to maximum the magnetic properties of single component SmCo_5 films, Fig. 6.[27] For the composites, smooth single phase type hysteresis loops were measured for both types of dispersed systems. This is illustrated in Figs. 7-9. SmCo_5 plus Al dispersions were made that exhibited room temperature coercivities of 15 kOe with ≈ 5 at.% Al and decreased to 5.7 kOe with 21 at.% Al. The SmCo_5 plus Al dispersions were only marginally affected by heating in air for 30 minutes to 300 °C, Fig. 10. It was possible to make SmCo_5 plus Co films with loop squareness of ≈ 0.83 and with room temperature coercivity ≈ 10 kOe by using a Co matrix.

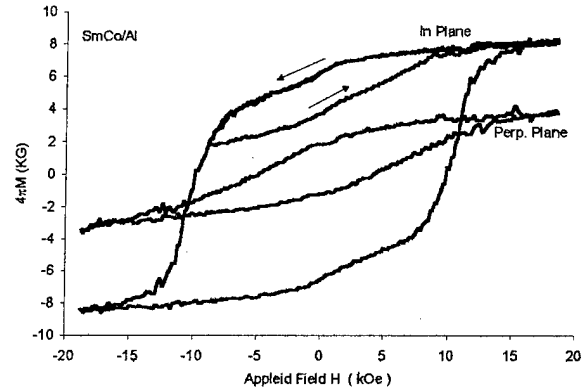


Fig. 7. Room temperature hysteresis loops are shown for a PLD SmCo_5 plus Al sputter film containing Sm 15.8 at.%, Co 74.5 at.%, and Al 9.7 at.%. The intrinsic coercivity was 9.9 kOe.[39]

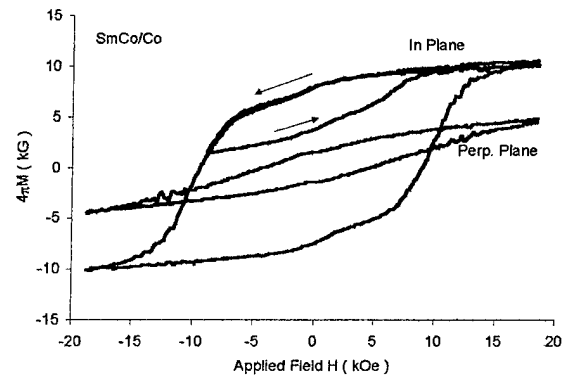


Fig. 8. Room temperature hysteresis loops are shown for a high coercivity PLD SmCo_5 sample plus simultaneous Co sputter deposition. The RT in plane intrinsic coercivity was 9.5 kOe.[39]

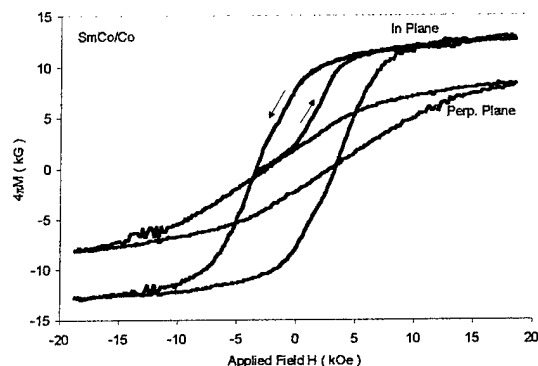


Fig. 9. Room temperature hysteresis loops are shown for a lower coercivity PLD SmCo_5 sample plus simultaneous Co sputter deposition. The RT in plane intrinsic coercivity was 3.4 kOe.[39]

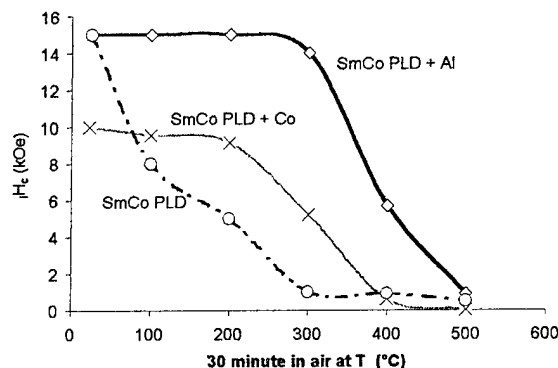


Fig. 10. The intrinsic coercivities measured at room temperature following heating for 30 minutes in air at various temperatures are shown for PLD SmCo plus Al films, diamonds, PLD SmCo plus Co, crosses, and PLD SmCo_5 only films, circles.[39]

A key feature of PLD is that it is a pulsed technique so that material is ablated from the targets during the laser pulse duration, ≈ 15 ns, which is short compared to the transit time of the ejected plume to the substrate.[37] A key feature of Ref.s 27,32, was that a specific laser pulse rate was required to allow sufficient surface mobility so that high coercivities could be obtained. The deposited material is thus aggregated into grains of a sufficiently small size

to exhibit high coercivities during the time between laser pulses. Shadow deposition was necessary to produce fully textured films with uniformly small grain sizes.

Figure 10 illustrates the corrosion resistance of PLD SmCo_5 nanodispersions in an Al or Co matrix and of PLD SmCo only films.[39] The samples with, ≈ 5 at.% Al, and without the Al matrix exhibited as deposited H_c of 15 kOe. The coercivity of the nanodispersed samples in Al remained largely unchanged after heating in air for 30 minutes at 300 °C. In contrast to this, the coercivities of the PLD SmCo_5 films, were rapidly deteriorated by heating in air to only 100 °C. Typically thin sputtered SmCo_5 films are readily deteriorated by even very short time heating in air at relatively low temperatures. In contrast to the SmCo/Al dispersions, the initial coercivity of the Co sample, 84 at.% Co, was 10.3 kOe versus 15 kOe for the PLD SmCo_5 film. The PLD SmCo_5 dispersions with Co started to lose intrinsic coercivity following heating in air for 30 minutes to 200 °C.

IV. Advances in Magnetoresistive Magnetic Memory Structures

Although $\text{La}_{0.7}\text{Sr}_{0.3}\text{MnO}_3$ bulk samples exhibit a ferromagnetic Curie point of 364 K,[40,41] the narrowness of the transition region as a function of temperature, and the high multi-Tesla magnetic field values required for saturating the magnetoresistance have precluded bulk applications. Over the last several years a number of groups have reported on transport properties for polycrystalline films. Such samples have been reported to exhibit a broadened resistance maximum as a function of temperature, T_P , at temperatures of approximately 200 to 250 K.[42-45] A key feature of the polycrystalline films was that the magnetoresistive response exhibited an enhanced low field as well as the normal high field magnetoresistivity. The magnetic properties of such polycrystalline films still exhibited bulk like behavior. In previous studies it was shown that films which exhibited a resistance maximum at 230 K, and low field MR response extending to above room temperature, still exhibited ferromagnetic hysteresis loops at room temperature with the actual ferromagnetic Curie temperature comparable to that of bulk $\text{La}_{0.7}\text{Sr}_{0.3}\text{MnO}_3$. [46] This is consistent with the polycrystalline films being comprised of grains exhibiting nearly bulk type magnetic behavior, and disordered grain boundary regions that strongly affect the film transport properties. Single crystal LaSrMnO films have been shown to exhibit anisotropic low field MR with the [001] and [110] directions respectively the easy

and hard directions.[47] Although $\text{La}_{0.7}\text{Sr}_{0.3}\text{MnO}_3$ crystallizes in SG 167 with $a = 5.506$ and $c = 13.356$ Å,[48] the simpler pseudocubic indexing with $a = 3.87$ Å has been used in this paper as was used in several recent papers.[47,49]

In this research we reported two new significant results that made it possible to construct a new type memory element using La-manganite films at room temperature. One was the synthesis of textured polycrystalline La,Sr-manganite films by high laser pulse energy, pulsed laser deposition, PLD. A key attribute of these films is that it has been possible to raise the temperature of the resistance maximum, T_P , to room temperature and above as a function of the laser pulse energy and deposition conditions. Films with room temperature T_P values were synthesized that exhibited either (110) or mixed (111) crystallite textures. The second result was that the low field MR of such polycrystalline film strips were highly anisotropic with respect to the current direction in the plane of the films and with respect to in plane versus out of plane magnetic fields.

Pulsed laser deposition, PLD, utilizing a Lambda Physik 305Fi excimer laser was used to deposit La-manganite films from a set of bulk compound targets. The films were deposited using a wavelength of 248 nm, with pulse energies from 500 to 1300 mJ, and by using a wavelength of 193 nm with laser pulse energies up to 600 mJ. Laser pulse rates from 5 to 50 Hz have been used. The estimated laser pulse width was 15 ns. A shadow mask has been used to shield part of the substrate during the PLD

process. In this manner, film regions of the same substrate deposited in and out of the shadow were studied. In these studies polished polycrystalline alumina substrates were used. In previous studies using 193 nm laser pulses at pulse energies of 500 mJ similar resistance versus temperature film response was observed for LaSrMnO films made onto polycrystalline alumina and c-plane sapphire substrates.[46] The films discussed here were deposited using a substrate temperature of 700-750 °C in 100 mTorr of flowing oxygen. The films were subsequently annealed in-situ in 200 Torr oxygen at the deposition temperature. Film thicknesses, grain sizes, and the presence of particulates has been studied using a scanning electron microscope, SEM. Film compositions were determined by electron excited x-ray spectroscopy in the SEM. The PLD target compositions were adjusted so that the shadow deposited films had the $\text{La}_{0.7}\text{Sr}_{0.3}\text{MnO}_3$ composition. Magnetization measurements were made using a vibrating sample magnetometer. Magnetoresistive measurements were made using a Hall probe for field determination to eliminate any hysteresis in the magnet system from shifting the zero applied magnetic field values. Certain LaSrMnO films were patterned by dry plasma etching.[50]

Resistances, normalized to the maximum value, versus temperature are shown in Fig. 11 for several high laser pulse energy PLD deposited LaSrMnO films.[51] Traces (c) and (d) are for shadow and non-shadow regions of the same substrate respectively. The shadow region, trace (c), exhibits the resistance

maximum at a temperature of 255 K, while for the non-shadow region, trace (d), the resistance maximum was at 155 K. This film was made with laser pulse energy of 1000 mJ, 248 nm, at 30 Hz with a substrate temperature of 750 °C. In this case there was a typical difference of 100 K between the temperature of the resistance maximum for the shadowed versus non-shadowed film regions. Films made using lower laser pulse energies of 500-600 mJ did not show such large differences in behavior between shadow and non-shadow film regions of the same substrate. Trace (b) exhibiting the broad resistance maximum at 326 K was for the shadow region of a similarly deposited film, but with a laser pulse energy of 1250 mJ at 30 Hz. Measurements made on this sample three months apart did not show any differences. Subsequent to removal from the deposition chamber, this sample was not heated above 385 K. Another sample, trace (a), initially exhibited the resistance maximum at 360 K. It should be noted that this is nominally the Curie point of bulk crystalline samples.² But upon heating to 406 K, the temperature of the resistance maximum decreased to 293 K and was subsequently stable upon recycling at that value.

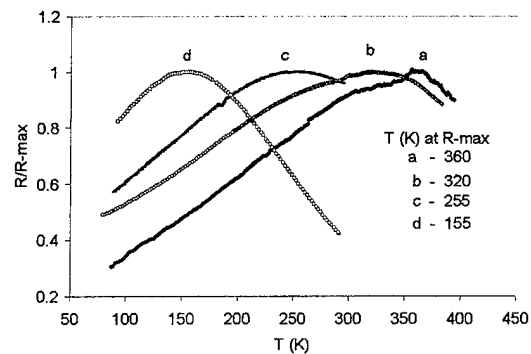


Fig. 11. This figure indicates the range of R vs T variation for high laser pulse energy LaSrMnO PLD deposited films. Traces (a),

(b), and (c) are for shadow deposited films at high laser pulse energies. Trace (d) was for the non-shadow deposited region of the same substrate as trace (c). The temperatures corresponding to the maximum resistance for each trace are indicated.[51]

Figure 12 shows x-ray diffraction traces, Cu K α radiation, for the shadow and non-shadow regions used for Fig. 11, traces (c) and (d). The shadow region of this sample made with high laser pulse energies was very strongly (110) textured. The non-shadow region was almost completely (111) textured. In a different series of films made similarly but at slightly higher deposition rates the shadow region was made to be mixed (111) and (110) textured. This is shown in the upper trace of Fig. 12. The substrates were polished polycrystalline alumina. The (110) texture of the shadow deposit corresponds to an appreciably longer stacking distance than the (111) texture of the non-shadow deposit regions. It should be noted that the growth rate of the non-shadow regions exceeds that of the shadowed region. This is consistent with more site relaxation time being required to facilitate the growth of the (110) texture mode as has been observed for sputtered films in other magnetic systems.[1] The T_p values for similarly prepared films were maximized for a laser pulse rate of 30 Hz. The laser pulse rate dependence was not as pronounced as for coercivity dependence of PLD SmCo films.[27] No evidence of preferential crystallite alignment within the plane of the film was observed. The use of shadow deposited PLD allowed a uniform and small grain size to be obtained in the films.

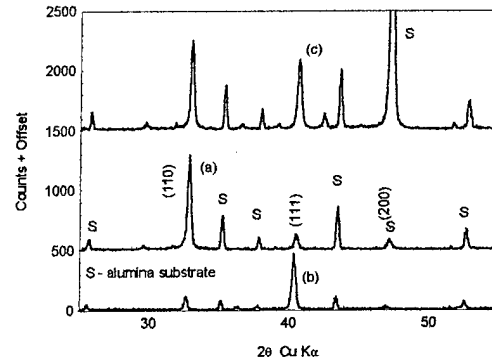


Fig. 12. X-ray diffraction traces are shown for the shadow, trace (a), and non-shadow regions, trace (b), corresponding to traces (c) and (d) respectively of Fig. 1. The shadow region trace has been displaced by 500 counts to separate the traces. Trace (c) is for the shadow region of a (110) and (111) mixed texture high pulse shadow deposited textured film. Trace (c) has been offset by 1500 counts. Peaks due to the polycrystalline alumina substrate are denoted by S.[51]

To test whether the films could be patterned for device applications, the films used for Fig. 11 traces (a) and (b) were dry etch patterned to make strips ≈ 100 microns wide by ≈ 1.5 and 2.5 mm length segments.[50] The film for Fig. 11 trace (b) after patterning exhibited the resistance maximum at a somewhat reduced temperature of 250 K. The film for Fig. 11 trace (a) after patterning exhibited a smooth resistance maximum at ≈ 292 K which was the same value as before patterning. The patterned film obtained from the Fig. 11(a) sample was deemed the most suitable for device applications since the resistance maximum was at nominally room temperature. This patterned film with a nominal resistance of $30 \text{ k}\Omega$ per mm length was used in a bridge circuit with comparable values to obtain the magnetoresistance data shown in Fig. 13. The low field magnetoresistive response was

distinctly greater when the applied magnetic field was directed in plane and parallel to the sample current than when in plane but perpendicular to the sample current. Demagnetization effects reduced the response for applied fields perpendicular to the plane to nearly zero for this applied field range. For these (110) textured films the easy direction of magnetizations of the crystallites were randomly aligned in the film plane and the magnetic hard axes were perpendicular to the film plane. The coercivity peaks at 2.6-3.0 mT are as expected. The arrows on Fig. 13 show that the response lagged the applied field. A new feature is the large degree of anisotropy in the low field MR for magnetic fields applied in plane parallel versus perpendicular to the sample current for these (110) textured polycrystalline films. A bridge output of 100 mV corresponded to a resistance change $\Delta R/R \approx 2.2\%$. No temperature compensation was used for measurements in the vicinity of room temperature. At a nominal bias field of 3 to 10 mT the in plane parallel to I sensitivity was 3.5 V/T.

Figure 14 shows the low field MR response for a mixed (111) and (110) textured LaSrMnO film corresponding to trace (c) in Fig. 11 with a T_p value of 269 K. The measurements were made at 293 K. In this case the response for low fields applied perpendicular to the plane was appreciable because many of the crystallite easy magnetization directions were skewed out of the film plane. The overall response in terms of $\Delta R/R$ was reduced, but still exhibited an enhanced response for fields applied parallel versus perpendicular to the current direction.

The magnetoresistance of the textured films has been shown to be strongly anisotropic with respect to magnetic fields applied in plane parallel to the current versus perpendicular to the current. The (110) textured films exhibited a greater low field MR than the (111) textured films, and were immune to perpendicular fields in the low field region.

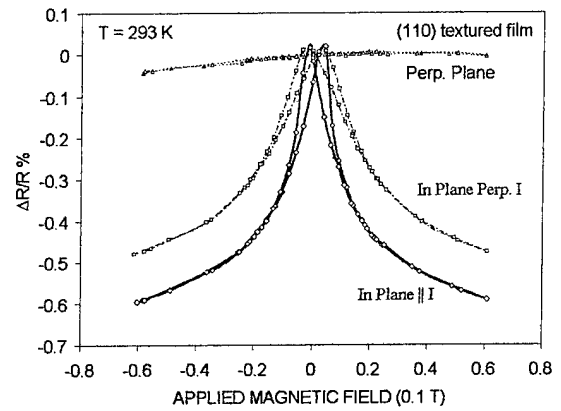


Fig. 13. The low field MR anisotropy for a (110) textured film is shown versus applied magnetic fields applied in plane, parallel and perpendicular to current, and perpendicular to plane as at measured at 293 K are shown. The curves were hysteretic with the peaks lagging the applied field values. A bridge output of 100 mV corresponds to a resistance change $\Delta R/R \approx 2.2\%$. [51]

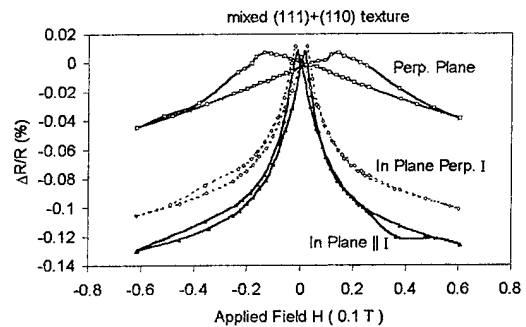


Fig. 14. The low field MR anisotropy for a mixed (111) + (110) textured film is shown versus applied magnetic fields applied in plane, parallel and perpendicular to current, and perpendicular to plane as at measured at 293 K. [51]

A prototype memory element was tested by placing a small bias magnet parallel to and above the magnetoresistive film strip to be electrically isolated from it.[52] Since the bias field was due to the looping field of the bias magnet, the direction of the bias field was opposite to that of the bias magnet itself. An external sweep magnetic field was then applied parallel to the strip and magnet. The geometry is shown by the inset in Fig. 15. As the external applied magnetic field was swept between plus and minus field values approaching the intrinsic coercivity of the bias magnet, the net magnetic field applied to the strip caused a highly nonlinear response for the LaSrMnO strip resistance. The bias magnet was measured to exhibit an intrinsic coercivity between 61 and 62 mT. The response of such a biased LaSrMnO film strip as measured at 292 K is shown in Fig. 15. In the figure the applied field has been cycled between ± 59 mT three times to demonstrate the stability of the results. It should be noted that the response is distinctly different from the case of a simple bias field that would simply translate the appropriate curve of Fig. 15 by the bias field value. A distinctive feature as shown by the arrows is that the maximum for positive field values occurs while the field is being reduced from positive values. For negative field excursions the maximum bridge response occurred at zero applied field. The position of the zero applied field is marked by the vertical line in Fig. 15. Field excursions to 58 mT parallel versus anti-parallel to the strip length produced zero applied field voltage levels separated by 13.2 mV in this case. The initial

magnetization direction of the bias magnet establishes which part of the trace represents the low and high voltage levels at $H = 0$.

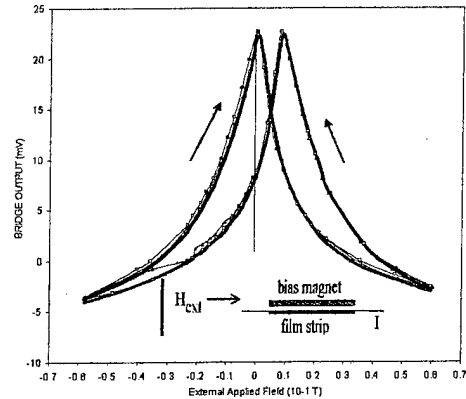


Fig. 15. The bridge output, cycled three times, versus applied magnetic field for a LaSrMnO patterned film strip biased by a small bias magnet parallel to the strip is shown. The inset shows that the film strip current, bias magnet, and external field are all aligned parallel to each other. The vertical line is located at the $H = 0$ position.

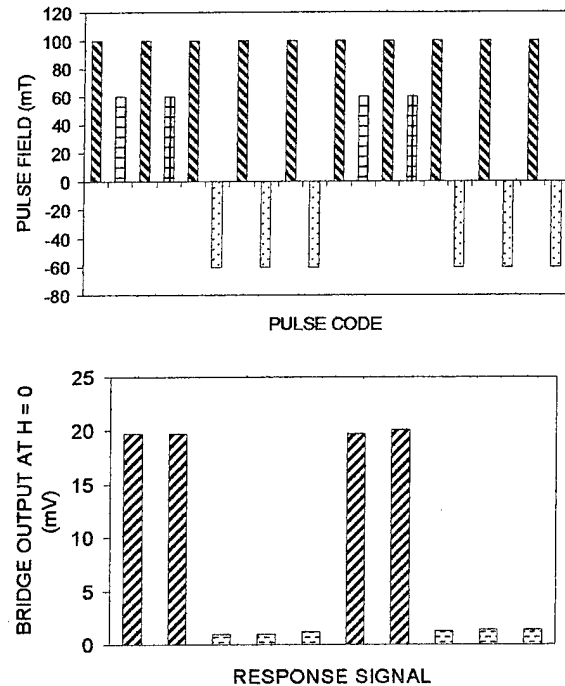


Fig. 16. The upper graph shows the pulse train of applied field values used to produce the zero applied field voltage state values of the lower panel. The zero applied field voltage levels differed by 18 mV.[52]

Stable and repeatable voltage level differences at zero applied field were obtained by using trailing pulse logic. In this mode of operation, the bias magnet was reset by a leading pulse exceeding the coercivity of the bias magnet, +100 mT here, which was followed by either a positive or negative applied field pulse of 60 mT. Representative pulse train values and the resulting memory state values are shown in Fig. 16. The value of the memory voltage following the coupled pulse pairs differed by 18 mV in the specified geometry. The memory state voltage was either high or low depending upon whether the trailing pulse had been +60 mT or -60 mT.

The magnetoresistance of the patterned (110) textured films has been shown to be strongly anisotropic with respect to magnet fields applied in plane parallel to the current versus perpendicular to the current, and to be immune to perpendicular fields in the low field region. Since the patterned LaSrMnO strip used in this bridge exhibited a broad resistance maximum as a function of temperature at 292 K, temperature compensation was not needed for room temperature operation. The introduction of a small interacting bias magnet, and in principle a

film magnet, oriented parallel to the strip resulted in a memory structure with separate zero field voltage levels depending upon whether the last applied field state had been parallel or anti-parallel. Stable repeatable memory states have been obtained by using trailing pulse logic in which the bias magnet state is reset by the leading pulse. The zero applied field memory states of the LaSrMnO biased film strip were non-volatile and persisted in the absence of any current flow. Consequently current would only need to be present during memory state poling. Thus low duty cycle operation would be anticipated.

Parts of this work concerning the deposition of La-manganite materials was supported by DARPA and the Office of Naval Research under contract ONR-N00014-96-1-0767. Support for the film deposition studies was from U. S. Army Research Office Grant No. DAAG55-98-1-0172. The La-manganite films used in the bridge construction were dry etch patterned by S. J. Pearton and F. Sharifi at the University of Florida.

V. The Growth of Particulate Free Films by a Newly Invented Deposition Method Using a Pulsed Laser

We began actively working on Pulsed Laser Deposition, PLD, for depositing high coercivity permanent magnet films in 1996 when our PLD facility was acquired through a NSF Academic Infrastructure Grant. Key aspects of this work required the use of shadowed pulsed laser deposition to restrict deposit to atomic species, and to the requirement of a very specific laser pulse repetition rate. It was demonstrated that μH_c values of 22 kOe could be achieved for fully crystallographically textured SmCo films made onto silicon and alumina substrates.[27] In April 2000 we began to actively work on methods to make PLD deposited films that would be free of particulates without the use of shadowing. On October 4, 2000 an invention disclosure titled "A Method for Making Films Utilizing A Pulsed Laser for Ion Injection and Deposition, PLID" was filed with the Research Foundation of CUNY, RF File No. 274. On January 17, 2001 a provisional patent application was filed by the Research Foundation of CUNY, Patent Serial Number 60/262051 titled "A Method for Making Films Utilizing a Pulsed Laser for Ion Injection and Deposition".[53] The basic invention uses a high pulse energy pulsed laser to generate a plume of ions, atom, and larger particulates. A combination of electrostatic and magnetic fields is then used to steer the high energy ions from this laser generated plume to a substrate region not in the direct line of sight of the plume. By this method the deposition consists of a beam of high energy ions that can be painted onto a specific substrate region by modulating the deflecting fields. Film adhesion of metals and other materials onto even room temperature substrates is very good. For example, very hard diamond like carbon films have been deposited onto room temperature glass substrates that are very hard to scratch by normal metal implements. An application we have been pursuing for these films is as tunneling barriers for magnetic tunnel junctions.

Magnetic tunnel junctions using metal oxide tunnel barriers have been widely investigated because of the attractive properties of aluminum oxide tunnel junctions.[54] Although aluminum oxide has many attractive features as a tunneling barrier, the optimum thickness is generally believed to be approximately 13 Å.[55] Typically metallic aluminum is deposited which is then oxidized, often with the aid of an electrical discharge. The required thinness of the oxide layer, and the necessity of introducing oxygen and subsequently removing it for the deposition of the top magnetic electrode, make it difficult to routinely manufacture oxide magnetic tunnel junctions. Other oxides such as Ta₂O₅ have been tested as tunnel barriers with lower values of $\Delta R/R$ reported than for Al₂O₃ barriers.[56,57] The semiconductor ZnS has also been reported to be usable but with $\Delta R/R$ only about 10 % at room temperature.[58] We have devised a method whereby thin particulate free diamond like carbon films can be made with good adhesion onto even room temperature substrates. The method employs a filtered ionized carbon beam created by the vacuum impact of a high energy, approximately 1 J per pulse, 248 nm excimer laser onto a carbon target.[53] The resultant deposition beam can be steered

and deflected by magnetic and electric fields to paint a specific substrate area. An important aspect of this deposition method is that the resultant films are particulate free and formed only as the result of atomic species impact. The carbon films exhibited the high hardness characteristic of diamond like carbon, DLC, films. Preliminary attempts have been made to use these particulate free DLC films for fabricating magnetic tunnel junctions.

Magnetic tunnel junctions have been formed by first using a metal contact mask to DC sputter deposit Cu and then Co strips 0.5 mm wide by 50 mm long onto polished alumina substrates. The Co was sputtered at a pressure of 5 mTorr Ar with a substrate temperature of 150 °C. The substrates were then transferred to a special pulsed laser deposition system in which magnetic and electrostatic deflection was used to vacuum deposit an ionized beam of carbon over the center part of the Co strip. Strong film adhesion was achieved due to the high ion kinetic energy of the carbon beam. The carbon film formed from the ionized carbon beam was particulate free and smooth. The carbon film thickness was tapered from one end to the other. Then seven equally spaced 0.5 mm wide permalloy, 81 at.% Ni 19 at.% Fe, cross strips were sputter deposited across the carbon strip. The permalloy stripe was then overlayed with Cu. At the cross strip intersections Cu-Co-DLC-PM-Cu magnetic tunnel junctions are then formed.

DLC films have been carbon ion deposited in vacuum onto various substrates including glass, silicon, and alumina. Even films deposited onto room temperature glass substrates exhibit strong adhesion and such films are difficult to scratch using normal metal tips. Figure 1 shows the optical constants for some DLC that were carbon ion deposited onto silicon substrates. The film hardness can be estimated by comparing the optical data for the laser generated ion beam films with the properties of DLC films deposited by filtered cathodic arc onto silicon substrates. The comparison of optical data of laser generated ion beam, LADLC, samples with cathodic arc, CADLC, shows that they are similar to "softer" CADLC labeled as "c-a_sft" in Fig. 17. The "softer" CADLC films have hardness of about 40-45 GPa and film stress about 4 – 5GPa. From the optical measurements the thickness of the LADLC deposited on silicon were determined to be: sample 051501 103 ± 10 Å, sample 051701 176 ± 10 Å. An a-Si boundary layer of 6-7 Å was also indicated to be present at the Si-LADLC interface. These measurements were made courtesy of Veeco Scientific Instruments, Plainview, NY. Scanning electron microscope examination of metallic films made by this laser induced ion beam method showed them to be particulate free. This is in decided contrast to films made by direct pulsed laser deposition that exhibit a high particulate density.

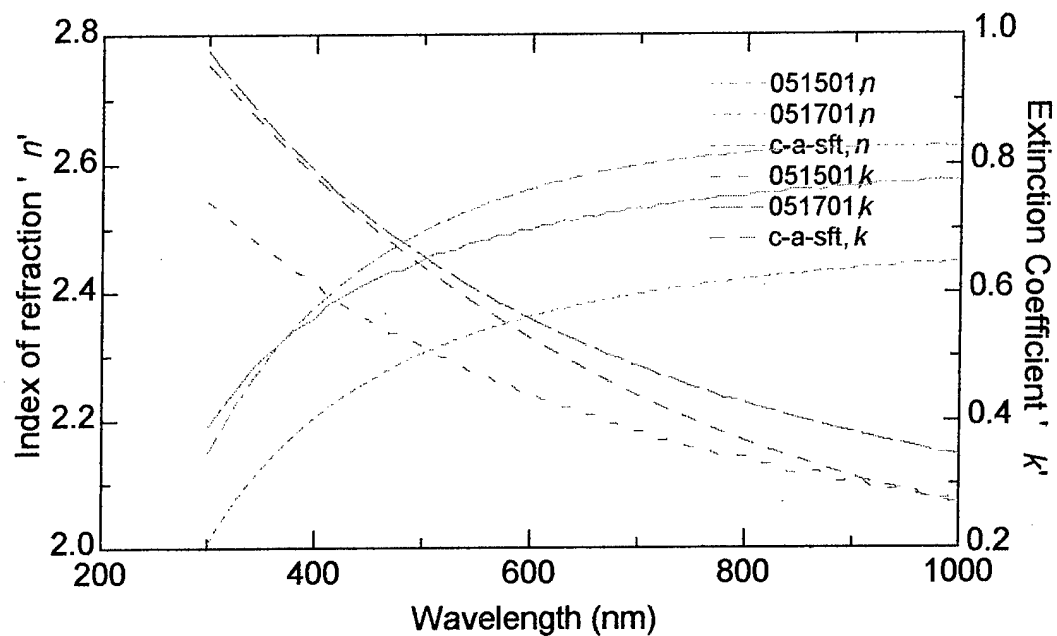


Fig. 17. Optical constants versus wavelength are shown for two laser carbon ion deposited films on silicon substrates, samples 051501 and 051701, along with a calibration film deposited by filtered cathodic arc deposition, a-sft.

Bibliography for Research Summary Section

1. F. J. Cadieu, Permanent Magnet Films for Applications, Chapter 1, Magnetic Film Devices volume of the Handbook on Thin Film Devices Technology and Applications, editors: J. Douglas Adam and Maurice H. Francombe, Academic Press, Inc., 2000.
2. F.J. Cadieu, pp. 179-189, Permanent Magnet Thin Films, in Physics of Thin Films, Vol. 16, (J. L. Vossen and M. Francombe, Eds.), Academic Press, San Diego, 1992.
3. F. J. Cadieu, H. Hegde, and K. Chen, Enhanced Crystal Texture Control For Sm-Co Based Films Sputtered In Ar-Xe Gas Mixtures, Thin Solid Films 193/194, 857 (1990).
4. Ref. 2, p. 178.
5. F.J. Cadieu, Permanent Magnet Thin Films, in Physics of Thin Films, Vol. 16, (J. L. Vossen and M. Francombe, Eds.), Academic Press, San Diego, 1992.
6. F. J. Cadieu, High Energy Product Permanent Magnet Films, in Magnetic Materials, Processes, and Devices IV, (L. T. Romankiw and D. A. Herman, Jr., Eds.), PV 95-18, p. 319-335, The Electrochemical Society Proceedings Series, Pennington, NJ (1996).
7. F. J. Cadieu, Selectively Thermalized Sputtering for the Deposition of Magnetic Films With Special Anisotropies, J. Vac. Sci. and Tech. A, 6, 1668 (1988).
8. F. J. Cadieu, H. Hegde, and K. Chen, The Synthesis of $\text{Sm}_2(\text{Co,Fe,Zr})_{17}$ High Energy Product, 16 to 30 MGOe, Thick Sputtered Films, IEEE Trans. on Magnetics, MAG-25, 3788 (1989).
9. F. J. Cadieu and Norbert Chencinski, Selective Thermalization in Sputtering to Produce High T_c Films, IEEE Transactions on Magnetics MAG-11, 227 (1975).
10. F. J. Cadieu, T. D. Cheung, S. H. Aly, L. Wickramasekara, and R. G. Pirich, Selectively Thermalized Sputtering for the Direct Synthesis of Sm-Co and Sm-Fe Ferromagnetic Phases, J. Appl. Phys. 53, 8338 (1982).
11. F. J. Cadieu, T. D. Cheung, S. H. Aly, L. Wickramasekara, and R. G. Pirich, Square Hysteresis Loop SmCo_5 Films Synthesized by Selectively Thermalized Sputtering, IEEE Trans. on Magnetics MAG-19, 2038 (1983).
12. F. J. Cadieu, T. D. Cheung, L. Wickramasekara, and S. H. Aly, Magnetic Properties of a Metastable Sm-Fe Phase Synthesized by Selectively Thermalized Sputtering, J. Appl. Phys. 55, 2611 (1984).
13. S. H. Aly, T. D. Cheung, L. Wickramasekara, and F. J. Cadieu, Directly Sputter Synthesized High Energy Product Sm-Co Based Ferromagnetic Films, J. Appl. Phys. 57, 2147 (1985).
14. F. J. Cadieu, T. D. Cheung, and L. Wickramasekara, Magnetic Properties of Sm-Ti-Fe and Sm-Co Based Films, J. Appl. Phys. 57, 4161 (1985).
15. F. J. Cadieu, T. D. Cheung, and L. Wickramasekara, Magnetic Properties of Sputtered Nd-Fe-B Films, J. Magn. Magn. Matl. 54-57, 535 (1986).
16. L. Wickramasekara, T. D. Cheung, and F. J. Cadieu, Large Perpendicular Anisotropy in Sputtered $\text{Sm}(\text{Ti,Fe})_2$ Films, J. Magn. Magn. Matl. 54-57, 1679 (1986).
17. T. D. Cheung, L. Wickramasekara, and F. J. Cadieu, Magnetic Properties of Ti Stabilized $\text{Sm}(\text{Co,Fe})_5$ Phases Directly Synthesized by Selectively Thermalized Sputtering, J. Magn. Magn. Matl. 54-57, 1641 (1986).

18. F. J. Cadieu, T. D. Cheung, L. Wickramasekara, and N. Kamprath, High $\mu_0 H_C$ Perpendicular Anisotropy Nd-Fe-B Sputtered Films, IEEE Trans. on Magnetics **MAG-22**, 752 (1986).
19. F. J. Cadieu, High Coercive Force and Large Remanent Moment Magnetic Films With Special Anisotropies, J. Appl. Phys. **61**, 4105 (1987).
20. N. Kamprath, N. C. Liu, H. Hegde, and F. J. Cadieu, Magnetic Properties and Synthesis of High $\mu_0 H_C$ Sm-Ti-Fe, J. Appl. Phys. **64**, 5720 (1988).
21. N. Kamprath, X. R. Qian, H. Hegde, and F. J. Cadieu, Magnetic Properties of Sm-Fe-Ti-Al Sputtered Films with $\mu_0 H_C$ Greater Than 30 kOe, J. Appl. Phys. **67**, 4948 (1990).
22. F. J. Cadieu, N. Kamprath, H. Hegde, K. Chen, A. Navarathna, and R. Rani, Analogous Sm-Fe-Ti High Coercivity Phases in Sm-Fe-V and Sm-Fe-Zr Sputtered Film Samples, J. Appl. Phys. **69**, 5608 (1991).
23. R. Rani, H. Hegde, A. Navarathna, and F. J. Cadieu, High Coercivity $Sm_2Fe_{17}N_x$ and Related Phases in Sputtered Film Samples, J. Appl. Phys. **73**, 6023 (1993).
24. F. J. Cadieu, H. Hegde, A. Navarathna, R. Rani, and K. Chen, High Energy Product $ThMn_{12}$ Sm-Fe-T and Sm-Fe Permanent Magnets Synthesized As Oriented Sputtered Films, Appl. Phys. Letters **59**, 875 (1991).
25. H. Hegde, X. R. Qian, Jong-Guk Ahn, and F. J. Cadieu, High Temperature Magnetic Properties of $TbCu_7$ -type SmCo Based Films, J. Appl. Phys. **79**, 5961 (1996).
26. M. Q. Huang, W. E. Wallace, M. McHenry, Q. Chen, and B. M. Ma, Structure and Magnetic Properties of $SmCo_{7-x}Zr_x$ Alloys ($x=0-0.8$), J. Appl. Phys. **83**, 6718 (1998).
27. F. J. Cadieu, R. Rani, T. Theodoropoulos, and Li Chen, Fully In Plane Aligned SmCo Based Films Prepared by Pulsed Laser Deposition, J. Appl. Phys. **85**, 5895 (1999).
28. Eric E. Fullerton, J. S. Jiang, Christine Rehm, C. H. Sowers, S. D. Bader, J. B. Patel, and X. Z. Wu, High Coercivity, Epitaxial Sm-Co Films with Uniaxial In-Plane Anisotropy, Appl. Phys. Lett. **71**, 1579 (1997).
29. F. J. Cadieu, H. Hegde, and K. Chen, High Energy Product Sm-Co Based Sputtered Films, Crystal Texturing and Magnetic Properties, J. Appl. Phys. **67**, 4969 (1990).
30. R. Rani, F. J. Cadieu, X. R. Qian, W. A. Mendoza, and S. A. Shaheen, SmCo Based Sputtered Films With $CaCu_5$ and $TbCu_7$ Structures, J. Appl. Phys. **81**, 5634 (1997).
31. H. Hegde, K. Chen, and F. J. Cadieu, Fe Enriched Sm-Co Based High Energy Product Sputtered Films With Precise Crystal Textures, J. Appl. Phys. **69**, 5850 (1991).
32. F. J. Cadieu, R. Rani, X. R. Qian, and Li Chen, High Coercivity SmCo Based Films Made By Pulsed Laser Deposition, J. Appl. Phys. **83**, 6247 (1998).
33. F. J. Cadieu, H. Hegde, E. Schloemann, and H. J. Van Hook, In-Plane Magnetized YIG Substrates Self Biased by SmCo Based Sputtered Film Coatings, J. Appl. Phys. **76**, 6059 (1994).
34. E. E. Fullerton, C. H. Sowers, J. P. Pearson, S. D. Bader, X. Z. Wu and D. Lederman, Appl. Phys. Lett. **69**, 2438 (1996).
35. H. Lemke, C. Echer, and G. Thomas, IEEE Trans. On Magn. **32**, 4404 (1996).
36. Choong Jin Yang, Sang Won Kim, and Jong Seog Kang, J. Appl. Phys. **83**, 6620 (1998).
37. Douglas H. Lowndes, D. B. Geohegan, A. A. Puretzky, D. P. Norton, C. M. Rouleau, Synthesis of Novel Thin-Film Materials by Pulsed Laser Deposition, Science **273**, 898 (1996).

38. J. C. S. Kools, Pulsed Laser Deposition of Metals, pp. 455-471, in Pulsed Laser Deposition of Thin Films, editors, Douglas B. Chrisey and Graham K. Hubler, Wiley, New York, 1994.
39. Li Chen, Biao Li, C. F. Cadieu, T. Theodoropoulos, and F. J. Cadieu, Nanophase Dispersed SmCo Films with High Remanence and Corrosion Resistance, *J. Appl. Phys.* **87**, 6128 (2000).
40. Yoshinori Tokura et al., *J. Phys. Soc. Japan* **63** (1994) 3931.
41. Y. Moritomo, A. Asamitsu, and Y. Tokura, *Phys. Rev. B* **51** (1995) 16491.
42. A. Gupta, G. Q. Gong, G. Xiao, P. R. Duncombe, P. Lecouer, P. Trouilloud, Y. Y. Wang, V. P. Dravid, and J. Z. Sun, *Phys. Rev. B* **54** (1996) R15 629.
43. H. Y. Hwang, S. -W. Cheong, N. P. Ong, and B. Batlogg, *Phys. Rev. Lett.* **77** (1996) 2041.
44. R. Shreekala, M. Rajeswari, K. Ghosh, A. Goyal, J. Y. Gu, C. Kwon, Z. Trajanovic, T. Boettcher, R. L. Greene, R. Ramesh, and T. Venkatesan, *Appl. Phys. Lett.* **71** (1997) 282.
45. X. W. Li, A. Gupta, Gang Xiao, and G. Q. Gong, *Appl. Phys. Lett.* **71** (1997) 1124.
46. F. J. Cadieu, R. Rani, X. R. Qian, C. F. Cadieu, Li, Chen, W. Mendoza, and S. A. Shaheen, Polycrystalline and Laminated $\text{La}_{0.7}\text{Sr}_{0.3}\text{MnO}_3$ Films Made By Pulsed Laser Deposition, *J. Appl. Phys.* **83** (1998) 7195.
47. Y. Suzuki and H. Y. Hwang, *J. Appl. Phys.* **85**, 4797 (1999).
48. P. G. Radaelli, G. Iannone, M. Marezio, H. Y. Hwang, S- W. Cheong, J. D. Jorgensen, and D. N. Argyriou, *Phys. Rev. B* **56**, 8265 (1997).
49. T. Walter, K. Dorr, K.-H. Muller, B. Holzapfel, D. Eckert, M. Wolf, D. Schlafer, L. Schultz, and R. Grotzschel, *Appl. Phys. Lett.* **74**, 2218 (1999).
50. J. J. Wang, J. R. Childress, S. J. Pearton, F. Sharifi, K. H. Dahmen, E. S. Gillman, F. J. Cadieu, R. Rani, X. R. Qian, and Li Chen, *J. Electrochem. Soc.* **145** (1998) 2512.
51. F. J. Cadieu, Li Chen, Biao Li, and T. Theodoropoulos, Enhanced Room Temperature Magnetoresistance Response in Textured $\text{La}_{0.7}\text{Sr}_{0.3}\text{MnO}_3$ Stripe Made by Pulsed Laser Deposition, *J. Appl. Phys.* **87**, 6770 (2000).
52. F. J. Cadieu, Li Chen, Biao Li, and T. Theodoropoulos, Room Temperature $\text{La}_{0.7}\text{Sr}_{0.3}\text{MnO}_3$ Magnetoresistive Prototype Memory Element, *Appl. Phys. Letters* **75**, 3369 (1999).
53. F. J. Cadieu, U. S. Provisional Patent No. 60/262051 titled "A Method for Making Films Utilizing a Pulsed Laser for Ion Injection and Deposition", Jan. 17, 2001.
54. S. Tehrani, B. Engel, J. M. Slaughter, E. Chen, M. DeHerrera, M. Durlam, P. Naji, R. Whig, J. Janesky, and J. Calder, Recent Developments in Magnetic Tunnel Junction MRAM, *IEEE Trans. Magn.* **36**, 2752 (2000).
55. Stuart A. Wolf and Daryl Treger, Spintronics: A New Paradigm for Electronics for the New Millenium, *IEEE Trans. Magn.* **36**, 2748 (2000).
56. P. Rottlander, M. Hehn, O. Lenoble, and A. Schuhl, Tantalum Oxide as an Alternative Low Height Tunnel Barrier in Magnetic Junctions, *Appl. Phys. Lett.* **78**, 3274 (2001).
57. M. F. Gillies, A. E. Kuiper, J. B. A. van Zon, and J. M. Sturm, Magnetic Tunnel Junctions with Tantalum Oxide Barriers Displaying a Magnetoresistance Ratio of Up to 10% at Room Temperature, *Appl. Phys. Lett.* **78**, 3496 (2001).
58. M. Guth, A. Dinia, G. Schmerber, H. A. M. van der Berg, Tunnel Magnetoresistance in Magnetic Tunnel Junctions with ZnS Barrier, *Appl. Phys. Lett.* **78**, 3487 (2001).

Papers Directly Resulting From This U. S. Army Research Grant

1. F. J. Cadieu, R. Rani, X. R. Qian, C. F. Cadieu, Li Chen, W. Mendoza, and S. A. Shaheen, Polycrystalline and Laminated $\text{La}_{0.7}\text{Sr}_{0.3}\text{MnO}_3$ Films Made By Pulsed Laser Deposition, *J. Appl. Phys.* **83**, 7195 (1998).
2. F. J. Cadieu, R. Rani, X. R. Qian, and Li Chen, High Coercivity SmCo Based Films Made By Pulsed Laser Deposition, *J. Appl. Phys.* **83**, 6247 (1998).
3. J. J. Wang, J. R. Childress, S. J. Pearton, F. Sharifi, K. H. Dahmen, E. S. Gillman, F. J. Cadieu, R. Rani, X. R. Qian, and Li Chen, Dry Etch Patterning of LaCaMnO_3 and SmCo Thin Films, *J. Electrochem. Soc.* **145**, 2512 (1998).
4. F. J. Cadieu, R. Rani, T. Theodoropoulos, and Li Chen, Fully In Plane Aligned SmCo Based Films Prepared by Pulsed Laser Deposition, *J. Appl. Phys.* **85**, 5895 (1999).
5. F. J. Cadieu, Permanent Magnet Films for Applications, Chapter 1 Magnetic Film Devices volume of the Handbook on Thin Film Devices Technology and Applications, editors: J. Douglas Adam and Maurice H. Francombe, Academic Press, Inc., 2000.
6. F. J. Cadieu, Li Chen, Biao Li, and T. Theodoropoulos, Room Temperature $\text{La}_{0.7}\text{Sr}_{0.3}\text{MnO}_3$ Magnetoresistive Prototype Memory Element, *Appl. Phys. Letters* **75**, 3369 (1999).
7. Li Chen, Biao Li, C. F. Cadieu, T. Theodoropoulos, and F. J. Cadieu, Nanophase Dispersed SmCo Films with High Remanence and Corrosion Resistance, *J. Appl. Phys.* **87**, 6128 (2000).
8. F. J. Cadieu, Li Chen, Biao Li, and T. Theodoropoulos, Enhanced Room Temperature Magnetoresistance Response in Textured $\text{La}_{0.7}\text{Sr}_{0.3}\text{MnO}_3$ Stripe Made by Pulsed Laser Deposition, *J. Appl. Phys.* **87**, 6770 (2000).
9. F. J. Cadieu, Li Chen, Biao Li, Enhanced Magnetic Properties of SmCo₅ Nanophase Composites Made by Simultaneous Pulsed Laser Deposition and Sputtering, Seventh International Conference on Composites Engineering, pp. 99-100, Denver, CO, July 2-8, 2000.
10. F. J. Cadieu, Li, Chen, and Biao Li, Enhanced Magnetic Properties of Nanophase SmCo₅ Film Dispersions, *IEEE Trans. On Magnetics*, **37**, 2570 (2001).

Invited Longer Papers, Book Chapters, and Review Articles

1. F. J. Cadieu, Permanent Magnet Films for Applications, Chapter 1 Magnetic Film Devices Volume of the Handbook on Thin Film Devices Technology and Applications, editors: J. Douglas Adam and Maurice H. Francombe, Academic Press, Inc., 2000.

D. Scientific Personnel

1. Professor F. J. Cadieu, Principal Investigator
2. Dr. Raj Rani, Research Associate
3. Dr. Biao Li, Research Associate
4. Dr. X. R. Qian, Research Associate
5. Mr. Theodore Theodoropolous, Queens College Masters Degree Student
6. Mr. Charles Cadieu, Intel High School Student
7. Mr. Li Chen, CUNY PhD Graduate Candidate
8. Mr. Joel Jacob, Queens College Undergraduate

E. Degrees Awarded as a Part of This Program

1. Mr. Theodore Theodoropolous, Queens College Masters Degree Student 1999
2. Mr. Charles Cadieu, High School Graduation, 2000, currently at MIT
3. Mr. Li Chen, PhD Degree anticipated January 2002

F. Report of Inventions (By Title Only)

F. J. Cadieu, U. S. Provisional Patent No. 60/262051 titled "A Method for Making Films Utilizing a Pulsed Laser for Ion Injection and Deposition", Filing Date, Jan. 17, 2001.